A Unique Case of Polymorphism in Polyiodide Networks Resulting from the Reaction of the Drug Methimazole and I_2.

M. Carla Aragoni,[a] Massimiliano Arca,[a] Francesco Demartin,[b] Alessandra Garau,[a] Francesco Isaia,[a,*] Vito Lippolis,[a] Tiziana Pivetta[a]

[a] Dipartimento di Scienze Chimiche e Geologiche, Università degli Studi di Cagliari, Cittadella Universitaria, 09042 Monserrato (CA), Italy. E-mail: isaia@unica.it

[b] Dipartimento di Chimica, Università degli Studi di Milano, via Golgi 19, 20133 Milano. Italy.

Abstract

The oxidation of thioamide methimazole ($C_4H_6N_2S$) with molecular diiodine in water afforded the ionic compound $[2(C_4H_5N_2S\text{-}SN_2C_4H_6)]I_3I_5$ (**1**) in **1-triclinic** and **1-monoclinic** polymorphs. The polymorphic nature of $[C_4H_5N_2S\text{-}SN_2C_4H_6]_2I_3I_5$ has been highlighted by comparing the structure of the **1-triclinic** form (CCDC-2242744) with that of the **1-monoclinic** form, reported in the literature. No significant geometric differences are observed for the cations in the two polymorphs. The polymorphism is essentially due to a different arrangement in the polyiodide network of the $[I_5]^-$ and $[I_3]^-$ components. The FT-Raman spectrum of **1-triclinic** shows the characteristic bands in the range 200–50 cm^{-1} which are in good agreement with the structural features of the polyiodide network. The molecular electrostatic potential maps of the cation methimazole-disulfide $[C_4H_5N_2S\text{-}SN_2C_4H_6]^+$ and the *bis*-cation methimazole-disulfide $\{[C_4H_5N_2S\text{-}SN_2C_4H_6]^+\}_2$ in **1-triclinic** have been studied to clearly identify the electrostatic potential energy distributions over the cations, and the electron belt and σ-hole areas responsible for the directionality of the non-covalent interactions in the polyiodides. It is suggested that the cation methimazole-disulfide may be a reaction intermediate in the inhibition of thyroid hormones by methimazole.

Introduction

The drug methimazole (1-methyl-imidazole-2-thione, $C_4H_6N_2S$)[1] (Chart 1) has been marketed for the treatment of thyroid diseases since the 1950s, following Atwood's studies on molecules with the thioamide function.[2] The mechanism of action of this drug has been the subject of numerous studies over the years, but no definitive conclusion has yet been reached on the mechanism of action. Uncertainty still exists as to which agent is the iodinating agent (I^+, I_2, OI^-, …) in the thyroid, and what interactions methimazole may have with these agents.[3]

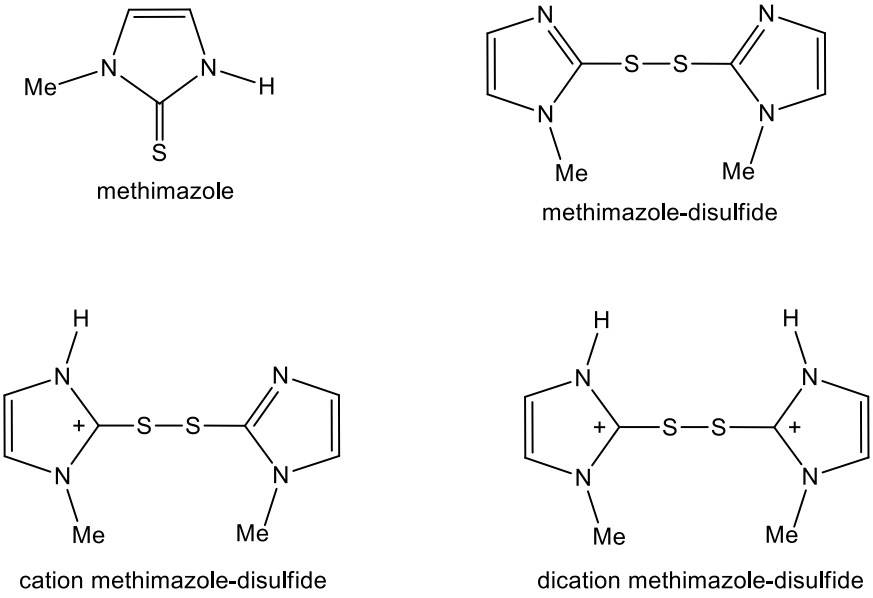

Chart 1. Formula schemes of compounds considered in this paper.

The apparently simple reaction between small molecules containing the thioamide function (DS) and I_2 reveals that the typology of the products obtained in the solid state is significantly influenced both by the intrinsic nature of DS as a Lewis base and by the reaction conditions (in particular: the polarity of the solvent and/or the molar ratio of the reagents). Consequently, the large number of X-ray characterised compounds reported in the literature reveals a varied and often unpredictable nature of the products obtained. A selection of classes of compounds identified in the solid state is shown in Scheme 1.

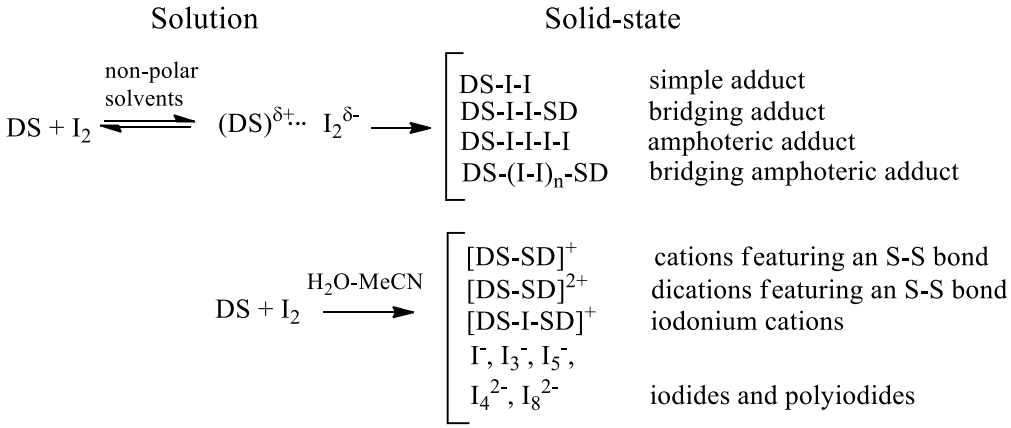

Scheme 1. Schematic representation of a selection of classes of compounds obtainable from the reaction of *S*-thioamide donor Lewis base (DS) and I_2. This scheme is intended to illustrate the different classes of compounds that can be obtained without implying the nature of the chemical bond involved.

Our research group has contributed to this topic over the last decades by studying the reactivity of sulphur-containing molecules of biological interest with diiodine, dihalogens and interhalogens and, where possible, by carrying out structural and spectroscopic characterisation of the various compounds obtained.[4] We have shown that the interaction of the drug methimazole ($C_4H_6N_2S$) with I_2 in polar solvents can lead to the oxidation of methimazole with the formation of the cation-methimazole-disulfide $[C_4H_5N_2S\text{-}SN_2C_4H_6]^+$ or the dication methimazole-disulfide $[C_4H_6N_2S\text{-}SN_2C_4H_6]^{2+}$, which can also be seen as different protonated forms of the neutral methimazole-disulfide $[C_4H_5N_2S\text{-}SN_2C_4H_5]$ (Chart 1). In particular, the reaction of methimazole with I_2 in water produced a black insoluble powder which, after recrystallization from CH_2Cl_2, yielded crystals of the salt $[C_4H_5N_2S\text{-}SN_2C_4H_6]_2I_3I_5$ (**1**), as identified by X-ray diffraction analysis in the monoclinic form (**1-monoclinic**).[4a] In the present study, we have further investigated the study of the reaction in water between methimazole and molecular diiodine using more controlled reaction conditions for the oxidation of methimazole. We report here the synthesis and the crystal structure of the triclinic polymorph (**1-triclinic**) of the salt $[C_4H_5N_2S\text{-}SN_2C_4H_6]_2I_3I_5$ (**1**), which to our knowledge represents a unique case of polymorphism in polyiodide networks. DFT calculations using the ωB97X-D/6-31G* basis set were performed to determine the charge densities on the cations and anions. The molecular electrostatic potential (MEP) maps are also discussed. Finally, some considerations on the role of the cation methimazole-disulfide (Chart 1) in the inhibition process of the *pro*-hormones monoiodotyrosine and diiodotyrosine by methimazole are reported.

Results and discussion

Reactivity of methimazole with I_2 in water.

The reaction in water between I_2 and methimazole was carried out by simultaneous mixing of identical volumes of dilute equimolar solutions of each reagent to maintain a molar ratio of the two species close to 1:1 throughout the mixing. The reaction resulted in the precipitation of a black powder accompanied by the formation of a small number of microcrystals, both characterised by an elemental analysis suitable for a methimazole/I_2 ratio of approximately 1:1. Crystallisation of the black powder in CH_2Cl_2 yielded the monoclinic form of $[C_4H_5N_2S\text{-}SN_2C_4H_6]_2I_3I_5$ (**1-monoclinic**), the X-ray crystal structure of which was briefly reported and discussed by us in a previous communication article.[4a] X-ray diffraction study of the microcrystals formed together with the black powder showed them to be the triclinic polymorph of the same compound (**1-triclinic**), (ESI-Table S1, -Table S2).

The overall reaction leading to the formation of both polymorphs can be written as follows:

4 (methimazole) + 5 I_2 → $[C_4H_5N_2S\text{-}SN_2C_4H_6]_2I_3I_5$ (**1**) + 2 HI

A possible oxidation pathway of methimazole in H_2O by I_2 is shown in Scheme 2. One diiodine molecule oxidises two methimazole molecules to give the methimazole-disulfide, two anions I^-, and two H^+ ions.[5] The subsequent mono-protonation of methimazole-disulfide leads to the formation of the cation methimazole-disulfide $[C_4H_5N_2S\text{-}SN_2C_4H_6]^+$.

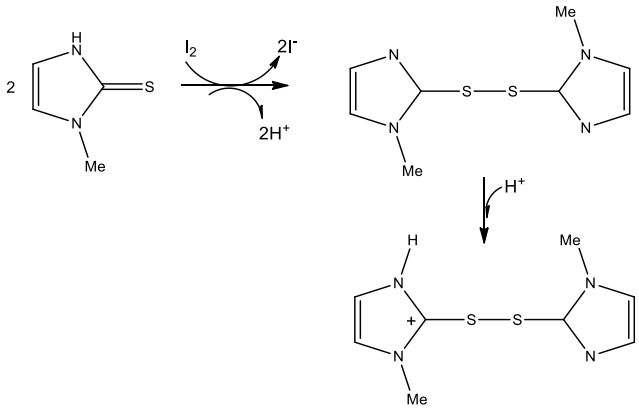

Scheme 2. Oxidation process of methimazole by I_2 in H_2O. Formation of the cation methimazole-disulfide $[C_4H_5N_2S\text{-}SN_2C_4H_6]^+$.

Crystal structure of (1-triclinic)

A view of the structure of the triclinic polymorph of $[C_4H_5N_2S\text{-}SN_2C_4H_6]_2I_3I_5$ (**1-triclinic**) (space group P-1), seen almost along [100], is shown in Figure 1. In the asymmetric unit there are two independent $[C_4H_5N_2S\text{-}SN_2C_4H_6]^+$ monocations interacting *via* hydrogen bonds to form a dimeric unit with a total charge 2+ (Figure 2). These cationic dimers $\{[C_4H_5N_2S\text{-}SN_2C_4H_6]^+\}_2$ are hosted within the poly-iodide framework, which is composed of pentaiodides and triiodides units (Figure 3). Each pentaiodide anion is close to a crystallographic inversion center and interacts with its symmetry related counterpart through its central iodine atom [I6···I6b distance of 3.8254(11) Å]. An analogous situation occurs for the triiodide anion, again close to another crystallographic inversion center, with an I3···I3a distance between the two symmetry-related triiodides of 3.8282(11) Å. Additional interactions below the sum of the van der Waals radii of iodine (about 4.20 Å)[6] are that between a pentaiodide and a triiodide [I1···I8 4.1238(10) Å] and that between two symmetry pentaiodides related by another inversion center [I4···I4c 3.5752(11) Å]. The triiodide anions are nearly symmetric and linear with an average I–I distance of 2.928 Å and an I1–I2–I3 angle of 178.98(2)°. The pentaiodide anions can be described as deriving from two diiodine molecules interacting with an I^-

anion, with two longer distances involving the central I^- [I5–I6 3.1134(9) and I6–I7 3.0207(8) Å] and two shorter [I4–I5 2.7936(9) and I7–I8 2.8255(8) Å] and an I5–I6–I7 angle of 96.26(2)°.

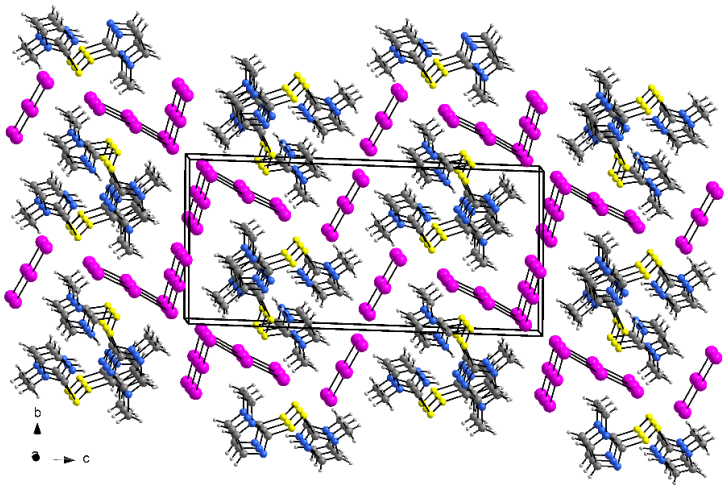

Figure 1. Perspective view of the triclinic polymorph of $[C_4H_5N_2S\text{-}SN_2C_4H_6]_2I_3I_5$ (**1-triclinic**) seen almost along [100].

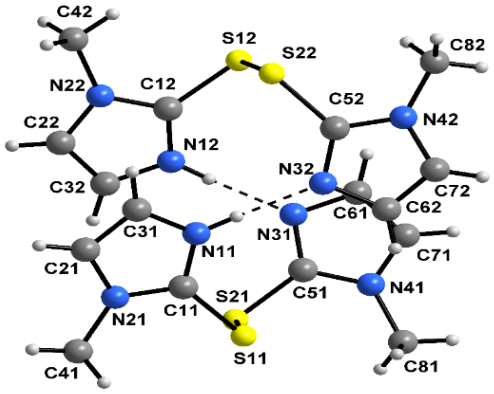

Figure 2. View of the $\{[C_4H_5N_2S\text{-}SN_2C_4H_6]^+\}_2$ dimeric unit formed by the two hydrogen-bonded independent $[C_4H_5N_2S\text{-}SN_2C_4H_6]^+$ cations in **1-triclinic**. N11–H···N32 2.690(9), N12–H···N31 2.712(8) Å.

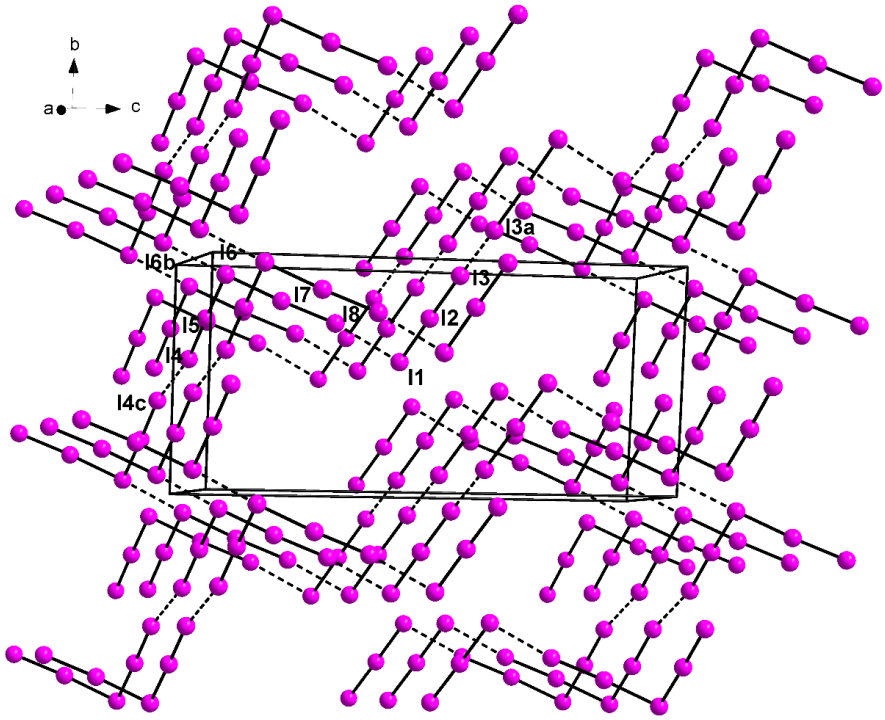

Figure 3. Polyiodide network in **1-triclinic**. I···I interactions below 4.2 Å are shown as dashed lines.

The polymorphic nature observed for $[C_4H_5N_2S\text{-}SN_2C_4H_6]_2I_3I_5$ (**1**) can be highlighted by comparing the structure of the triclinic form with that of the monoclinic one.[4a] From Figures 1 and 4 it is clear that the polymorphism is essentially due to the different polyiodide network. The asymmetric unit of **1-monoclinic** also contains two independent $[C_4H_5N_2S\text{-}SN_2C_4H_6]^+$ cations, but in this case they are located around two different two-fold axes at 1/2, y, 3/4 and 0, y, 1/4, respectively, and do not interact with each other through N-H···N hydrogen bonds, but with their symmetry equivalent; giving rise to two different dimeric units, each with a total charge 2+ each (Figure 5). The charge balance is achieved by the presence of $[I_5]^-$ and $[I_3]^-$ ions in the general position. The pentaiodides are essentially arranged in layers stacked along the [010] direction and interact each other with I···I contacts of 3.681 Å (Figure 6). The triiodides are located almost normal to these layers with I···I contacts with the pentaiodides of 3.66 and 4.28 Å. The resulting tridimensional polyiodide network shows channels along [100] and [001] where the dimeric cationic units are hosted (ESI-Figure S1).

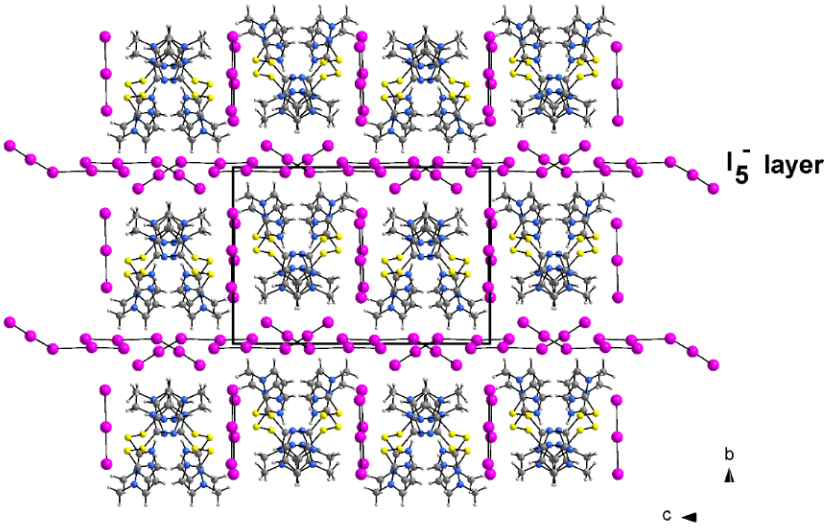

Figure 4. Perspective view of the monoclinic polymorph of $[C_4H_5N_2S\text{-}SN_2C_4H_6]_2I_3I_5$ (**1-monoclinic**) seen along [100].

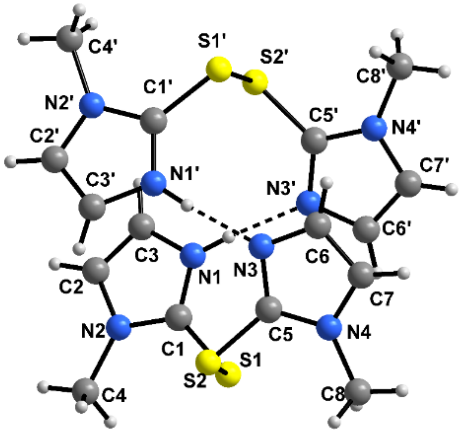

Figure 5. One of the two independent $[C_4H_5N_2S\text{-}SN_2C_4H_6]^+$ monocations of the asymmetric unit present in **1-monoclinic**, interacting *via* hydrogen bonding with its symmetry-related counterpart (a crystallographic two-fold axis relates the two molecules) to give a dimeric dication.

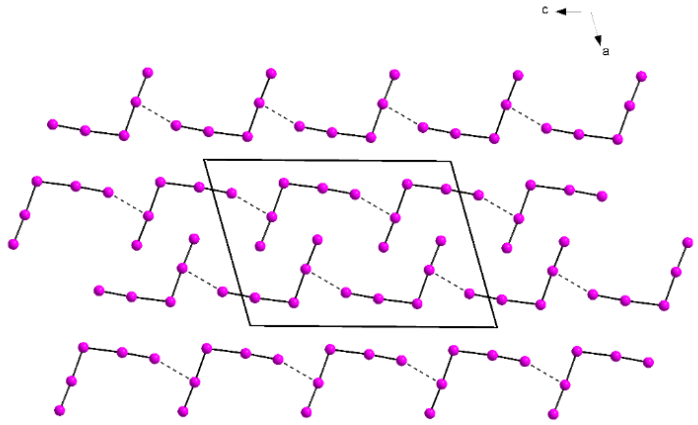

Figure 6. Partial view of a layer of $[I_5]^-$ in **1-monoclinic** seen along [010]. I···I contact of 3.681 Å, below the sum of the van der Waals radii (4.200 Å), are shown as dashed lines.

Structure analysis of **1-triclinic** shows that the two methimazole units, A (*N*-protonated), and B (*N*-non-protonated) (Figure 7), linked by a disulfide bond, have different bond distances.

For example, the C–S– (thiol) bond length of 1.739(7) and 1.750(7) Å observed in A and B, respectively (ESI-Table S2), is slightly longer than the C=S (thione) bond of 1.682/1.686 Å found in methimazole.[7a] Also the bond distances in unit A of N11–C11, C11–N21 (1.317 and 1.341 Å, respectively) and in unit B of N31–C51, C51–N41 (1.317 and 1.346 Å, respectively) are shorter than in methimazole (1.348, 1.358 Å) due to the increased conjugation of the electronic lone pairs on the nitrogen atoms to the CS carbon atom.

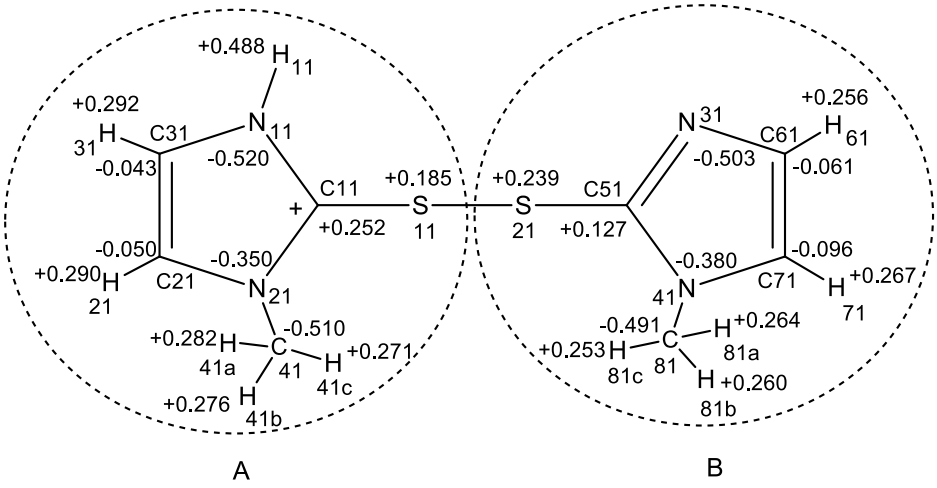

Figure 7. Cation methimazole-disulfide: atom numbering scheme; electron density (e) (see also ESI-Table S3); selected bond lengths: C11–S11 1.739(7), C11–N11 1.317(8), C11–N21 1.341(8), N11–C31 1.350(9), N21–C211.354(10), C21–C31 1.350(11), S11–S22 2.088(3), C51–S21 1.750(7) , C51–N31 1.317(8), C51–N41 1.346(8), N31–C61 1.357(10), N41–C71 1.341(10), C61–C71 1.342(11) Å; N11–C11-N21 107.3(6), N31–C51–N41 111.1(6) °.

Determination of the electronic charges of the elements by density functional theory (DFT) calculations shows that the +1 charge of the cation methimazole-disulfide is unequally distributed between the A and B units, +0.86 e and +0.14 e, respectively (ESI-Figure S2, ESI-Table S3). In unit A the C–S– group and all C–H hydrogens have higher positive values than the corresponding elements in unit B **(**C + S charges in C–S bonds: +0.437 e *vs* +0.366 e in units A and B, respectively; Hs charges in C–H bonds, +1.411 e *vs* +1.300 e, in units A and B, respectively). Noteworthy is the significant charge difference between the two units due to the N–H hydrogen contribution (+0.488 e) in A (Figure 7).

All the atoms involved in the disulfide fragment C11–S11–S21–C51 have a positive charge density with values of +0.252, +0.185, +0.239 and +0.127 |e| respectively. Conversely, the other elements forming the rest of the imidazole framework have a negative charge distribution: N11/N31 -0.520/-0.503, N21/N41 -0.350/-0.380, C31 /C61 -0.043/-0.061, and C21 /C71 -0.050/-0.096 |e|.

The *bis*-cation methimazole-disulfide $\{[C_4H_5N_2S\text{-}SN_2C_4H_6]^+\}_2$ (see ESI-Figure S3, ESI-Table S4 for the calculated charge distribution) is characterised by the presence of two intermolecular hydrogen bonds N11–H···N32 (2.690(9) Å) and N12–H···N31 (2.712(8) Å), respectively, (Figure 2) connecting the mono cation units. Neglecting basis set superposition errors, the calculated energy gain of the *bis*-cation methimazole-disulfide process formation from two cation methimazole-disulfide units is $E_{bis\text{-cat.}} - 2\ E_{mono\text{-cat.}} = 121.140$ kJ/mol.

In the *quasi*-symmetric triiodide ion I1–I2–I3, the charge is concentrated on the terminal iodine atoms I1 and I3 (-0.440 e, -0.485 |e|, respectively) while the central iodine I_2 is practically neutral (-0.019 |e|). In the V-shaped pentaiodide ion I4–I5–I6–I7–I8, the apical iodine I6 has a charge of -0.344 |e|, the rest of the charge is distributed between the terminal iodine atoms I4 (-0.281 |e|) and I8 (-0.341 |e|), while the iodine atoms I5 and I7 are considered almost neutral (ESI-Figure S5, ESI-Table S5).

Molecular electrostatic potential (MEP) maps

The electrostatic potential $V(\mathbf{r})$ generated in the space around a molecule by its nuclei and electrons is a useful indicator for interpreting and/or predicting its chemical reactivity. It has proved particularly useful in the analysis of non-covalent interactions such as hydrogen bonding.[8] The electrostatic potential $V(\mathbf{r})$ is a physical observable that can be determined computationally.[8b] It is now common practice to calculate it at the DFT level and analyse $V(\mathbf{r})$ (kJ/mol) on an appropriate three-dimensional electron density surface of the molecule, called $V_S(\mathbf{r})$ to indicate areas of electron excess and

deficiency. These are usually represented by different colours: red indicates the region with the most negative potential, while blue indicates the most positive region. In the case of cationic or anionic species, the colour scale reflects the range between the minimum and maximum value of the electrostatic potential energy present. [8c]

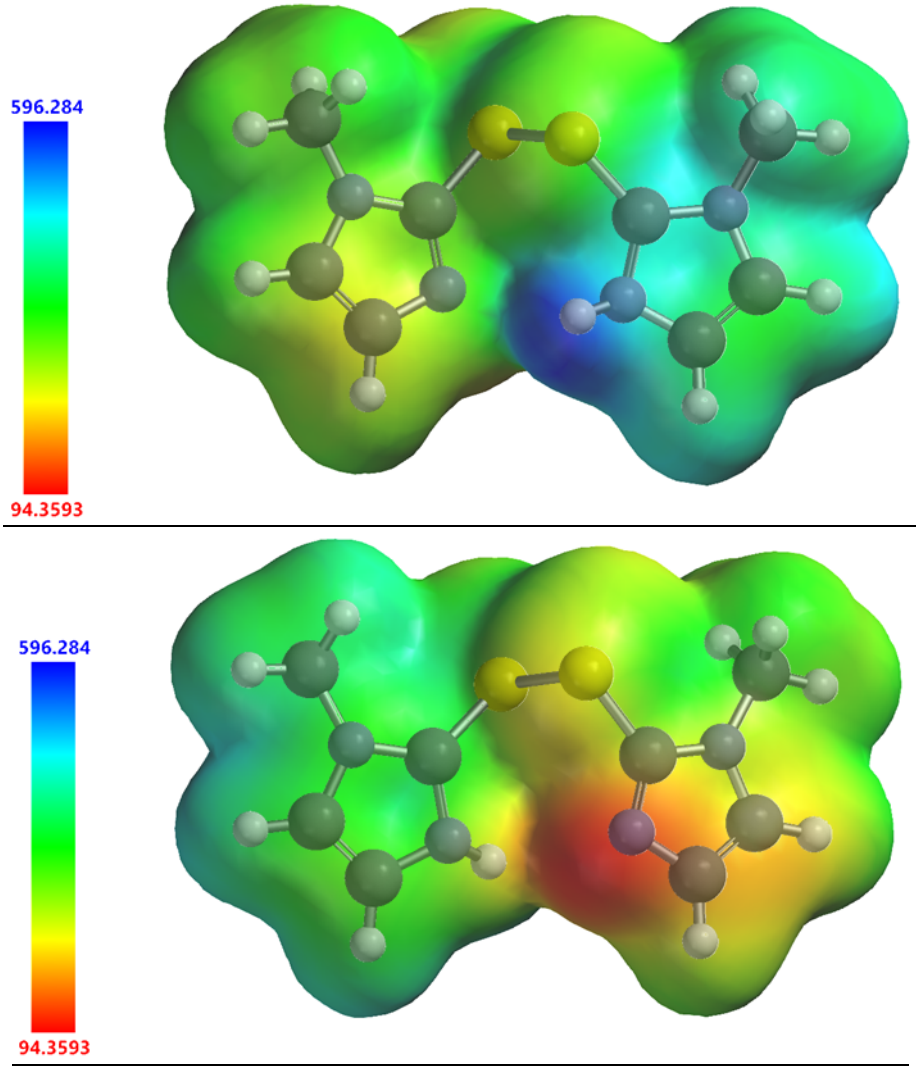

Figure 8. Views of the molecular electrostatic potential (MEP) map of the cation methimazole-disulfide, calculated at the ωB97X-D/6-31G* level, mapped onto the 0.002 au isodensity surface. The colour ranges, in kJ/mol, are from red (94.3) to blue (596.2).

The MEP maps of the cation methimazole-disulfide (Figure 8, and ESI-Figure S2) show that the electrostatic potential, which ranges from 94 to 596 kJ/mol, is distributed over the whole molecule. The lower energy value ($V_{S,min}$) refers to the area (dark blue) above the nitrogen N3, while the hydrogens in N–CH–CH–N and in the NCH_3 group show light blue areas. The upper value of the electrostatic potential ($V_{S,max}$) (red colour) refers to the area above the N1H group. The energy

difference $V_{S,max}$ - $V_{S,min}$ between the NHs (acting as hydrogen bond donors) and N3/N (acting as hydrogen bond acceptors) allows the formation of an NH···N hydrogen bond between two cation units,[8a] as it is found in the crystal-packing of the *bis*-cation methimazole-disulfide (Figure 9).
With the formation of the hydrogen bonds, the difference between the potentials at the nitrogens N1H and N3, which are the driving-force of the non-covalent interaction, is reduced[8b] (from 155 kJ/mol in the cation methimazole-disulfide to 117 kJ/mol in the *bis*-cation methimazole-disulfide, see ESI-Figure S3, ESI-Table S4).

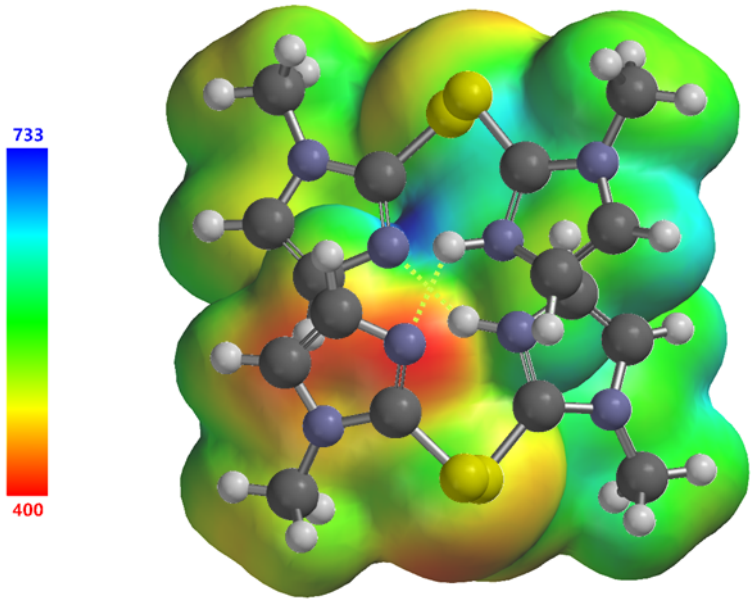

Figure 9. The molecular electrostatic potential (MEP) map of the *bis*-cation methimazole-disulfide, calculated at the ωB97X-D/6-31G* level, has been mapped onto the 0.002 au isodensity surface. MEP range 400–733 kJ/mol.

With regard to the anions in the **1-triclinic** compound, the charge in the slightly asymmetric $[I_3]^-$ I1–I2–I3 shows similar values for the terminal iodine atoms (-0.440 and -0.495 |e| in I1 and I3, respectively) and a value of -0.019 |e| for the central one. The V-shaped $[I_5]^-$ I4–I5–I6–I7–I8 can be described as the apical iodine I6 perturbing the iodine molecules I4–I5 and I7–I8 bound to it. The iodine I6 has a charge of -0.344 |e|, the rest of the negative charge is distributed between the terminal iodine atoms I4 (-0.281 |e|) and I8 (-0.341 |e|); the iodine atoms I5 and I7 can be considered almost neutral.
The MEP map of $[I_3]^-$ shows distinct regions with electrostatic potential values ranging from -320 kJ/mol (deep blue) to -420 kJ/mol (red). The least negative electrostatic potential characterises the tip of the terminal iodine atoms (-324.9 and -322.0 kJ/mol), an area known as the σ-hole which plays an important role in the strength and directionality of the secondary interaction.[9]

The more negative energy regions (red areas) form an area known as the 'electronic belt' around the iodine atoms I1 and I3, perpendicular to the σ-hole. The electrostatic potential energy values of the electron belt, for the iodine atoms I1 and I3, are -418.2 and -413.0 kJ/mol, respectively. For iodine I2, whose surface is bounded on both sides by the two electron belts, the value is -402.2 kJ/mol (orange colour). When an I_2 molecule is involved in a donor-acceptor interaction, there is an elongation of the I–I bond with respect to that observed in crystalline I_2 (2.715 Å).[7b] As a result, there is a redistribution of the electronic density, leading to an anisotropy in the electrostatic potential of the molecule.[9]

In the MEP map of $[I_5]^-$, all iodine atoms in the perturbed molecules I4–I5 and I7–I8 show the electron belt (-321.0, -344.0. kJ/mol and -324.1, -359.2 kJ/mol, respectively), and on the terminal iodine I4 and I8 the σ-hole regions (-208.2 and -198.3 kJ/mol, respectively) (Figure 10 and ESI-Figures S4 and S5, -Table S5). The highest value of the molecular electrostatic energy is found on iodine I6 (-360.0 kJ/mol), in an area perpendicular to the plane of the anion. The σ-hole on I4 and I8 makes these areas suitable for to the formation of non-covalent interactions with electron-rich species.[9c,d] This observation is reflected in the crystal packing of the compound **1-triclinic,** where an attractive electrostatic interaction between the σ-hole of iodine I4 of a pentaiodide anion and the electron belt of the terminal iodine I1 (donor) of the adjacent triiodide, results in an L-shaped arrangement [4.123(8) Å].

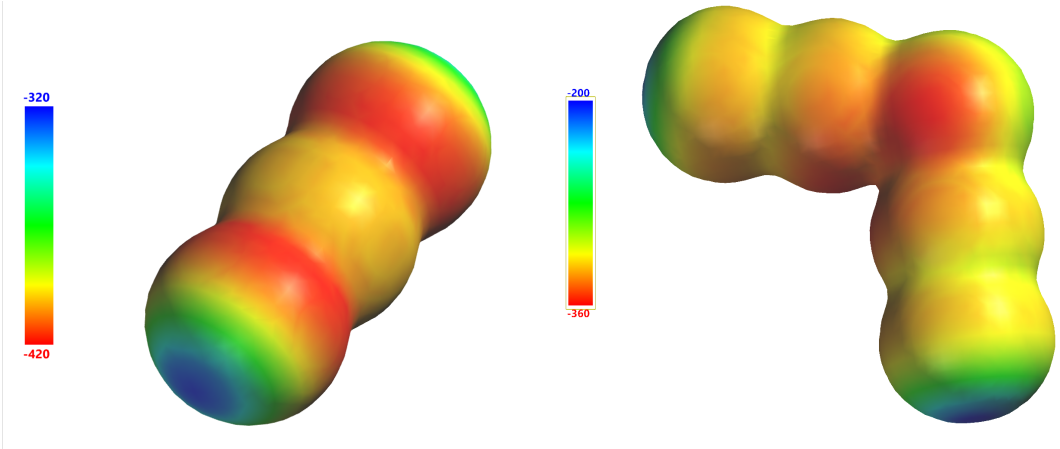

Figure. 10. The molecular electrostatic potential (MEP) map of the anions $[I_3]^-$ and $[I_5]^-$, calculated at the ωB97X-D/6-31G* level, has been mapped onto the 0.002 au isodensity surface.
MEP range -420 – -320 kJ/mol.

FT-Raman spectroscopy

FT-Raman spectroscopy is a powerful tool for the study of compounds with I–I bonds. FT-Raman spectroscopy allows the identification of typical polyiodide species such as triiodide, pentaiodide and molecular iodine in donor-acceptor systems.[10]

Since the structural data of the **1-triclinic** and **1-monoclinic** polymorphs were available, we thought it would be interesting to record the Raman spectrum of these compounds in order to characterise them further.

The I_3^- ions can be divided into two types, symmetric or asymmetric according to the bond distances in the two *d*(I–I).[11] In the linear and symmetric $[I_3]^-$ ion, the only Raman-active mode is the symmetric stretching (ν_1) which occurs around 110 cm^{-1}. In the case of the asymmetric $[I_3]^-$ ion, in addition to the Raman mode (ν_1), the bending deformation (ν_2) and the antisymmetric stretching (ν_3) become Raman-active. The values of (ν_3) and (ν_2) are found around 134 and 80 cm^{-1}, respectively. In the case of highly asymmetric $[I_3]^-$ ions, these can be considered as weak adducts between I^- (donor) and I_2 (acceptor) $[I^-\cdot(I_2)]$, in which case the Raman mode, observed at 180 cm^{-1} in I_2(s), is expected to shift to lower frequencies (typically in the range of 180–140 cm^{-1}). [10]

The $[I_5]^-$ pentaiodides occur in three different forms: V-shaped $[I^-\cdot(I_2)_2]$, L-shaped $[I_3]^-\cdot(I_2)$, and linear $[I^-\cdot(I_2)_2]$. Consequently, each type of pentaiodide will have a corresponding Raman spectrum as originating from the discrete units $[I_3]^-$ and/or I_2.[11]

In the **1-triclinic** and **1-monoclinic** polymorphs, the triiodide ion I1–I2–I3 shows a difference in the two *d*(I–I) distances of 0.0513 Å, and 0.006 Å, respectively. This indicates that there are two types of triiodide ion: asymmetric in the **1-triclinic** and symmetric in the **1-monoclinic**. The $[I_5]^-$ polyiodide unit in the **1-triclinic** and **1-monoclinic** compounds (iodine atoms I4–I8) is characterized by the iodine I6, which interacts with the molecules I4–I5 and I7–I8. The bond distances in I6–I5 (3.113 Å and 3.118 Å, respectively) and I6–I7 (3.020 and 3.245 Å, respectively) are indicative of a V-shaped $I^- \rightarrow 2(I_2)$ type system with an angle I5–I6–I7 of 96.35° in **1-triclinic** and 100.87° in **1-monoclinic**. Solid-state FT-Raman spectra of the **1-triclinic** and **1-monoclinic** compounds (Figure 11) were recorded in the 50-500 cm^{-1} region. They show a series of bands below 250 cm^{-1} the assignment of which have been assigned according to the above considerations. In the **1-triclinic** compound the bands at 112 and 132 $cm^{-1}$are assigned to the (ν_1) and (ν_3) modes of the asymmetric $[I_3]^-$ ions. The band at 160 and the shoulder at 172 cm^{-1} can be attributed to the ν_1(I–I) stretching vibration of the perturbed diiodine molecules I(7)–I(8) (*d* = 2.8255 Å) and I(5)–I(4) (*d* = 2.7936 Å), which together with iodine I6 form the V-shaped $[I_5]^-$ ion. For the **1-monoclinic** compound, the band at 113 cm^{-1} is assigned to the stretching mode (ν_1) of the

symmetric $[I_3]^-$ ion. The bands at 153 and 166 cm^{-1} are related to the ν_1(I–I) stretching vibration of the diiodine molecules I7–I8 (d = 2.742 Å) and I4–I5 (d =2.811 Å) slightly perturbed by the interaction with iodine I6.

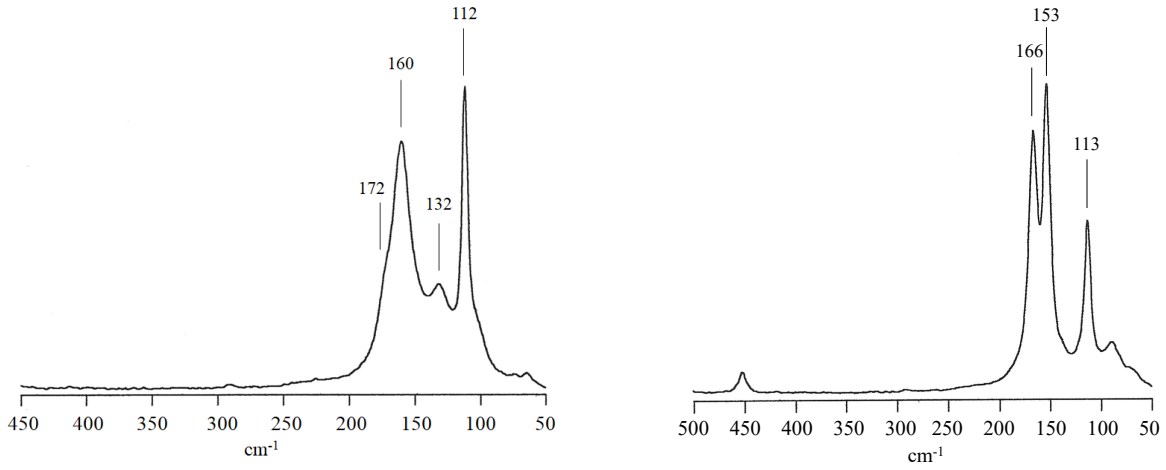

Figure. 11 Raman spectra in the range 500-50 cm^{-1}. Left: compound **1-triclinic**. Right: compound **1-monoclinic**.

Conclusions

The reaction of thioamide methimazole in water with molecular iodine (molar ratio 1:1) leads to the formation of the solid compound $[C_4H_5N_2S\text{-}SN_2C_4H_6]_2I_3I_5$ (**1**) in two polymorphic forms **1-triclinic** and **1-monoclinic**. The use of a polar solvent promotes a redox process leading to the oxidation of the thioamide group and the formation of iodide ions. These can interact with free iodine in solution, if present, to form triiodide, pentaiodide, or more complex polyiodide species in the solid state.[11] To the best of our knowledge, this is the first example of polymorphism in extended polyiodide networks resulting from a different 3D spatial arrangement of the same basic constituents ($[I_3]^-$ and $[I_5]^-$ ions).

In both polymorphs the monocations $[C_4H_5N_2S\text{-}SN_2C_4H_6]^+$ are arranged to form dimeric units held together by hydrogen bonds with an overall 2+ charge. Such units are formed by two independent monocations in **1-triclinic** whereas in **1-monoclinic** we have two different dications formed by a couple of two-fold symmetry-related monocations. No significant geometrical differences features are observed for the cations in the two polymorphs. It is evident that the polymorphism is essentially due to a different polyiodide network. In **1-triclinic** we observe channels, hosting the dications, extending along [100] formed by triiodides normal to [011] and pentaiodides stacked along [100]. In **1-monoclinic** the pentaiodides are essentially arranged in layers stacked along the [010] direction and the triiodides are located almost normal to these layers. The resulting

tridimensional iodide framework shows channels along [100] and [001] where the dimeric cationic units are located.

Several studies have shown that methimazole can inhibit thyroid peroxidase (TPO) directly, and that it can act as a competitive substrate for TPO *in vivo*, becoming iodinated itself and interfering with thyroglobulin iodination. In the latter case methimazole proceeds with the formation of the intermediate methimazole-disulfide which subsequently evolves into 1-methylimidazole, sulfate, sulfite, and other products (Scheme in ESI)[1b,c,2d]. As the cation methimazole-disulfide, together with the dication methimazole-disulfide are species closely related to methimazole-disulfide, it is possible to hypothesise that they may play some role in the mechanism of inhibition of TPO-catalysed iodination by methimazole. The possibility of polymorphism in their polyiodide salts increases the possibility of a fine tuning in the inhibitory effects of methimazole.

Experimental

All reactants and solvents were used as purchased from Aldrich. The concentration of iodine-saturated solution in water (1.142×10^{-3} M, $T = 20$ °C) was standardized against sodium thiosulfate 0.05 M titration.[13] FT-Raman spectra were recorded as solid samples on a Bruker FRS 100/s Fourier transform Raman spectrometer, operating with a diode-pumped Nd:YAG excitation laser emitting at 1064 nm.

Synthesis of the $[(C_4H_5N_2S\text{-}SN_2C_4H_6)]_2I_3I_5$ polymorphs 1-triclinic and 1-monoclinic. Solutions in water of methimazole (52.0 mg, 4.568×10^{-4} mol, 400 mL) and I_2 (116.0 mg, 4.568×10^{-4} mol, 400 mL) at $T = 20$ °C were added simultaneously, 10 mL at a time, to 50 mL of H_2O over a period of 2 hr to 50 mL of H_2O to give a reddish solution. The solution was then allowed to stand for 2 days at $T = 10$ °C and filtered through a G3 glass filter. Small dark red crystals (**1-triclinic**) were collected along with a dark red powder, washed with H_2O and stored at low temperature. Compound (**1-triclinic**): Yield: 0.0174 g, 13.0 % $C_{16}H_{22}I_8N_8S_4$ M (1469.85 g/mol): calcd % C 13.07, H 1.51, N 7.62, S 8.72. Found: C 13.0, H 1.4, N 7.5, S 8.5. Crystals of (**1-monoclinic**) were obtained by crystallization of the dark red powder from CH_2Cl_2 (30 mL) and slow evaporation of the solvent at low temperature. Yield: 0.069 g, 52.0 % $C_{16}H_{22}I_8N_8S_4$ M (1469.85 g/mol): calcd % calcd % C 13.07, H 1.51, N 7.62, S 8.72. Found: C 12.9, H 1.4, N 7.4, S 8.6.

X-ray structure determination of 1-triclinic

A summary of the crystal data and refinement details for the triclinic polymorph of $[2(C_4H_5N_2S\text{-}SN_2C_4H_6)]I_3I_5$ is given in ESI-Table S1. Intensity data were collected at room temperature on a Bruker Apex II CCD diffractometer using graphite-monochromatized Mo-Kα radiation (λ = 0.71073 Å).

Datasets were corrected for Lorentz-polarization effects and for absorption (SADABS)[14]. The structure was solved by direct methods (SIR-97)[15] and completed by iterative cycles of full-matrix least squares refinement on Fo^2 and ΔF synthesis using the SHELXL-2017[16] program (WinGX suite)[17]. Hydrogen atoms, located on the ΔF maps, were also included in the structure model riding on the atom to which they are attached. Selected interatomic distances, angles, torsion angles and hydrogen bonds are reported in the supplementary information ESI-Table S2. Crystallographic data have been deposited with the Cambridge Crystallographic Data Centre as supplementary publication no. CCDC-2242744. These data can be obtained free of charge fromwww.ccdc.cam.ac.uk/conts/retrieving.html (or from CCDC, 12 Union Road, Cambridge CB2 1EZ, UK; fax: +44 1223 336033; e-mail: deposit@ccdc.cam.ac.uk.

Computational studies

The geometry of the molecules was optimized on an Intel-i9 based system using Spartan'20 (Wavefunction Inc.) by DFT calculations using the ωB97X-D density functional, including a Grimme's dispersion correction term[18] and the split-valence 6-31G* as the basis set. Relativistic effective core potentials were adopted for heavy atoms. IR frequency calculations were performed to verify the nature of the minima at each optimisation step, by evaluating the absence of calculated negative frequencies. Heat of formation, electron density surface, atomic, electrostatic,[19] natural,[20] and Mulliken charges,[21] and the HOMO and LUMO energies were also calculated.

Conflicts of interest

There is no conflict to declare

References

1. The antithyroid drug methimazole is currently the mainstay of pharmacological treatment for Graves' disease in Europe, Japan and the United States, and has become the most commonly prescribed antithyroid drug over the past 20 years. The most widely accepted mechanism of action of methimazole is to inhibit the production of the thyroid hormones thyroxine (T4) and triiodothyronine (T3) by the thyroid gland. Methimazole interferes with the process that causes the iodination of tyrosine residues in thyroglobulin, mediated by the enzyme thyroid peroxidase, by acting as an alternative substrate to the iodinating species. (*a*) A. B. Emiliano, L. Governale, M. Parks and D. S. Cooper, *J. Clin. Endocrinol. Metab*., **2010**, 5(5), 2227–2233; (*b*) D. S. Cooper, *N. Engl. J. Med.,* **2005**, 352, 905–917; (*c*) E. B. Burch, D. S. Cooper, *European Journal of*

Endocrinology, **2018**, 179, R261-R274; (*d*) D. Manna, G. Roy, G. Mugesh, *Accounts of Chemical Research*, **2013**, 46(11), 2706-2715.

2. (*a*) E. B. Astwood, *Harvey Lecture*, **1945**, 40, 195–245; (*b*) E. B. Astwood, *JAMA,* **1984**, 251, 1743–1746; (*c*) M. M. Stanley, E. B. Astwood, *Endocrinology*, **1949**, 44, 588; (*d*) A. Taurog, *Endocrinology*, **1976**, 98, 1031–1046; (*e*) B. Davidson, M. Soodak, J. T. Neary, H. V. Strout, J. D. Kieffer, H. Mover, F. Maloof, *Endocrinology*, **1978**, 103, 871–882; (*f*) D. S. Cooper, *New England Journal of Medicine*, **2005**, 352, 905–917; (*g*) D. Manna, G. Roy, Mugesh, *Accounts of Chemical Research*, **2013**, 46, 2706–2715.

3. (*a*) H. Engler, A. Taurog, M. L. Dorris, *Endocrinology* **1982**, 110, 190–197; (*b*) F. Monaco, C. Santolamazza, I. De Ros, A. Andreoli, *Acta Endocrinology*, **1980**, 93, 32–36; (*c*) Taurog, M. L. Dorris, F. S. Guziec, *Endocrinology*, **1989**, 124, 30-39; (*d*) D. Doerge (U.S. Patent 5,371,102, year 1994).

4. (*a*) M. C. Aragoni, M. Arca, F. Demartin, F. A. Devillanova, A. Garau, F. Isaia, V. Lippolis, G. Verani. *J. Am. Chem. Soc.,* **2002**, 124, 4534-4539; (*b*) F. Isaia, M.C. Aragoni, M. Arca, F. Demartin, F. A. Devillanova, G. Floris, A. Garau, M. B. Hursthouse, V. Lippolis, R. Medda, G. Verani, *J. Med. Chem.,* **2008**, 51, 4050-4053; (*c*) V. Lippolis and F. Isaia, Charge-Transfer (C.-T.) adducts and Related Compounds, in Handbook of Chalcogen Chemistry: New Perspectives in Sulfur, Selenium and Tellurium, ed. F. Devillanova and W.-W. du Mont, 2nd edn, **2013**, ch. 8.2, vol. 1, pp. 448–472; (*d*) R. Montis, M. Arca, M. C. Aragoni, A. Bauzà, F. Demartin, A. Frontera, F. Isaia, V. Lippolis, *CrystEngComm.,* **2017**, 19, 4401-4412;

5. T. S. Lobana, R. Sultana, R. J. Butcher, A. Castineiras, T. Akitsu, F. J. Fernandez, M. C. Vega, *Eur.J.Inorg.Chem*., **2013**, 5162-5170.

6. F. H Allen, D. G. Watson, L. Brammer, A. G. Orpen, R.Taylor (**2006**) Typical interatomic distances: organic compounds. In: Prince E. (eds) International Tables for Crystallography Volume C: Mathematical, physical and chemical tables. International Tables for Crystallography, vol C. Springer, Dordrecht.

7. (*a*) The unit cell of methimazole contain two-crystallographically-independent molecules linked by as hydrogen-bonded pairs. G. Vampa, S. Benvenuti, F. Severi, M. Malmusi, N. Antolini, *J. Heterocyclic Chem*. **1995**, *32*, 227–234; (*b*) F. von Bolhuis, P. B. Koster, T. Migchelsen, *Acta Crystallogr*., **1967**, 23, 90-91.

8. (*a*) P. Politzer, J. S. Murray, Z. Peralta-Inga*, Int. J. Quantum Chem.,* **2001**, 85, 676-684.; (*b*) J. S. Murray, P. Politzer, *WIREs Comput. Mol. Sci.*, **2011**, 1, 153-163; (*c*) K. S. Ken, P. Politzer, *J.*

Chem. Phys., **1989**, 90, 4370-4372; (*d*) T. Clark, *Faraday Discuss*., **2017**, 203, 9-27; (*e*) T. Clark, P. Politer, J. S. Murray, *WIREs Comput Mol Sci*, **2015**, 5:169-177.

9. (*a*) G. Cavallo, P. Metrangolo, R. Milani, T. Primati, A. Primigi, G. Resnati, G. Terraneo, *Chem. Rev.,* **2016**, 116, 2478-2601; (*b*) M. V. Chernysheva, M. Bulatova, X. Ding, M. Haukka, *Cryst. Growth & Des*., **2020**, 20(11) 7197-7210; (*c*) T. Clark, *Faraday Discuss*., **2017**, 203, 9-27; (*d*) M. Savastano, *Dalton Trans.,* **2021**, 50, 1142-1165.

10. (*a*) P. Klaboe, *J. Am. Chem. Soc.* **1967**, 89, 15, 3667–3676; (*b*) P. Deplano, F. A. Devillanova, J. R. Ferraro, F. Isaia, V. Lippolis, M. L. Mercuri, *Appl. Spectrosc*., **1992**, 46, 1625-1629; (*c*) M. Arca, M. C. Aragoni, F. A. Devillanova, A. Garau, F. Isaia, V. Lippolis, A. Mancini, G. Verani, Bioinorganic Chemistry and Applications, Volume 2006, Article ID 58937, Pages 1-12.

11. Almost all polyiodides are constructed from I^-, $[I_3]^-$ and I_2 units, displaying a strong tendency to form extended motifs by means of halogen bonds. (*a*) H. Svenson, L. Kloo, *Chem Rev*., **2003**, 103(5), 1649-1684; (*b*) E. M. Nour, L. H. Chen, J. Laane, *J. Phys. Chem*., 1986, 90, 13, 2841- 2846; (*c*) I. D. Yushina, B. A. Kolesov, E. V. Bartashevich, *New J. Chem.,* **2015**, 39, 6163-6170; (*d*) A. J. Blake, F. A. Devillanova, R. O. Gould, W. S. Li, V. Lippolis, M. Schroder, *Chem. Soc. Rev.,* **1998**, 27, 195-206; (*e*) K. Sonnenberg, L. Mann, F. A. Redeker, B. Schmidt, S. Riedel, *Angew. Chem. Int. Ed.*, **2020**, 59(14), 5464-5493.

12. Experimental evidences do not support the formation of polyiodide ions such as $[I_5]^-$, $[I_7]^-$ … *etc*. in solution. V. T. Calabrese, A. Khan, *J. Phys. Chem. A*., **2000**, 104, 1287-1292

13. J. Mendham, R. C. Denney, J. D. Barnes and M. J. K. Thomas, Vogel's Quantitative Chemical Analysis, Prentice Hall, New York, 6th edn, 2000, pp. 428-460

14 SADABS Area-Detector Absorption Correction Program, Bruker AXS Inc. Madison, WI, USA, 2000.

15 A. Altomare, M. C. Burla, M. Camalli, G. L. Cascarano, C. Giacovazzo, A. Guagliardi, A. G. G. Moliterni, G. Polidori, R. Spagna, *J. Appl. Cryst.,* **1999**, 32, 115-119.

16. G. M. Sheldrick, Crystal structure refinement with SHELXL. *Acta Crystallogr., Sect. C*: *Struct, Chem*., **2015**, *71*, 3-84)

17. L. J. Farrugia, *J. Appl. Crystallogr.,* **1999**, 32, 837-838.

18. S. Grimme, J. Antony, S. Ehrlich and H. Krieg , *J. Chem. Phys.*, 2010, **132**, 154104.

19. M. Breneman and K. B. Wiberg, *J. Comput. Chem.*, 1990, **11**, 361-373

20. A. E. Reed, R. B. Weinstock and F. Weinhold , *J. Chem. Phys.*, 1985, **83** , 735-746.

21. (*a*) R. S. Mulliken, *J. Chem. Phys.*, 1955, **23**, 1833-1840; (*b*) R. S. Mulliken, *J. Chem. Phys.*, 1955, **23**, 2338-2342.